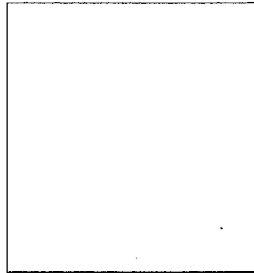


RECENT B-PHYSICS RESULTS FROM CDF

D. BORTOLETTO

*Department of Physics, Purdue University,
West Lafayette IN, USA*



Between 1992 and 1996 CDF collected about 100 pb^{-1} of data at a $\sqrt{s} = 1.8 \text{ TeV}$ at the Fermilab Tevatron collider. This data sample led to a large number of precision measurements of b hadrons properties including their masses, lifetimes and neutral B meson oscillation parameters and the discovery of the B_c meson. Here I report on three recent results: the measurement of the B^+ production cross section, the search for radiative penguin B hadron decays and the measurement of the CP violating parameter $\sin 2\beta$. These results are significant examples of the breadth of the CDF program. In 2001 the main injector will allow the Tevatron initially to deliver 1 fb^{-1} per year at $\sqrt{s} = 2 \text{ TeV}$. The CDF detector will undergo major upgrades which will further increase the b physics reach.

1 Introduction

Hadronic machines have historically played an important role in the study of the properties of b quarks. The most appealing feature of a hadronic machine is that the b production cross section is very large. The production cross section at the Tevatron collider is $\approx 100 \mu\text{b}$ at $\sqrt{s} = 1.8 \text{ TeV}$ while it is 1.1 nb at the $\Upsilon(4S)$ resonance. Unfortunately b events are only a small fraction of the overall event rate and therefore the signal-to-background is only of the order 10^{-3} . The challenge is to devise a trigger system which suppresses the background by three order of magnitudes. The simplest technique to enhance the b content is to trigger on high momentum leptons. During run 1 CDF triggered on B hadrons using semileptonic decays ($b \rightarrow \ell X, \ell = e, \mu$) or $B \rightarrow J/\psi X, J/\psi \rightarrow \mu^+ \mu^-$.

Hadronic machines offer unique possibilities with respect to b-factories operating at the $\Upsilon(4S)$. They are a unique laboratory to study heavy quark production in Quantum Chromo Dynamics (QCD). Moreover, B_s^0 and B_c^+ mesons and b baryons are not produced at a b-factory operating at the $\Upsilon(4S)$.

Herein, I present three recent results from CDF which are the latest measurement of the B production cross section, the search for radiative penguin decays and the first attempt to measure $\sin 2\beta$ at a hadron collider. These measurements are excellent examples of the richness of the b physics program covered by CDF from the study of QCD to the CP violation in b decays. The results are based on the analysis of 110 pb^{-1} collisions at \sqrt{s} of 1.8 TeV , collected between August 1992 to February 1996, which we refer to as Tevatron Run I.

The Tevatron will resume $p\bar{p}$ collisions in the Spring 2001 at $\sqrt{s} = 2.0 \text{ TeV}$. This future data taking period is referred to as Run II. The expected data rate is 2 fb^{-1} in the first two years of operation which corresponds to approximately $10^{11} b\bar{b}$ pairs per year. The Tevatron will continue to operate beyond these first two years and a data sample of more than 15 fb^{-1} will be collected before the turn-on of the LHC.

2 The CDF Detector

The features of the Run I CDF detector¹ crucial for B physics included a four-layer silicon microstrip detector (SVX), a large volume drift chamber (COT), and excellent electron and muon identification. The silicon microstrip detector provided an impact parameter (d_0) resolution for charged tracks of $\sigma(d_0) = (13 + 40/p_T) \mu\text{m}$, where p_T is the magnitude of the component of the momentum of the track transverse to the beam line in units of GeV/c . This impact parameter resolution made the precise measurement of B hadron proper decay times, t , possible. The drift chamber was 1.4 m in radius and was immersed in a 1.4 T axial magnetic field. It provided excellent momentum resolution $(\delta p_T/p_T)^2 = (0.0066)^2 + (0.0009 p_T)^2$ (where p_T is in units of GeV/c) and excellent track reconstruction efficiency making it possible to fully reconstruct B hadron decays with excellent mass resolution and a high signal to noise ratio. Electron (e) and muon (μ) detectors in the central rapidity region ($|y| < 1$) made it possible to detect and trigger on B hadrons using semileptonic decays ($b \rightarrow \ell X, \ell = e, \mu$) or $B \rightarrow J/\psi X, J/\psi \rightarrow \mu^+ \mu^-$.

3 The measurement of the B Cross Section

QCD can be used to compute the expected cross sections for the production of heavy quarks at hadron collider energies. Calculations of the hard-scattering cross section have been carried out to next-to-leading order in perturbation theory². It is imperative to show that these predictions provide an adequate description of the cross section at 1.8 TeV before they can be confidently extrapolated to higher energies or more exotic phenomena.

CDF has recently updated the measurement of the B production cross section which was published in 1993³. The new measurement uses the complete Run 1 data sample of $(98.1 \pm 4.0) \text{ pb}^{-1}$. Special care has been taken to minimize the systematic uncertainties and to remove biases. We use only the decay mode $B^+ \rightarrow J/\psi K^+$ and require both muon candidates from the J/ψ decay to be well measured by the silicon vertex detector. Such a restriction allows us to use fewer selection cuts since the decay mode $B^+ \rightarrow J/\psi K^+$ has a good signal-to-background ratio. Moreover, several of the efficiencies are

measured using a large sample of $\approx 86,000$ J/ψ candidates rather than relying on Monte Carlo for detailed modeling of occupancy related effects.

To select charged B candidates we considered each charged particle track as a kaon candidate to be combined with the J/ψ . A cut on the kaon transverse momentum of $p_T > 1.25$ GeV/ c is imposed to reduce the large combinatorial background due to soft p_T particles from the underlying event. The muon and kaon tracks are constrained to come from a common point of origin and the mass of the $\mu^+ \mu^-$ pair is constrained to the known J/ψ mass. The p_T of each B^+ candidate is required to be greater than 6 GeV/ c . The proper decay length is required to be greater than 100 μm to suppress backgrounds associated with prompt J/ψ mesons.

To measure the B^+ meson differential cross section as a function of p_T , the candidate mass distributions are divided into four p_T ranges: 6-9, 9-12, 12-15, and 15-25 GeV/ c . The number N_{sig} of B^+ mesons is determined using an unbinned maximum likelihood fit to a Gaussian signal function plus a linear background. The differential cross section $d\sigma/dp_T$ is calculated with the following equation:

$$\frac{d\sigma(B^+)}{dp_T} = \frac{N_{sig}/2}{\Delta p_T \cdot \mathcal{L} \cdot A \cdot \epsilon \cdot \mathcal{B}} \quad (1)$$

where the width of the p_T bin is Δp_T and \mathcal{L} is the integrated luminosity of the sample. The geometric and kinematic acceptance A is determined by a Monte Carlo simulation and includes the kinematic and trigger efficiencies. The efficiency ϵ is the additional reconstruction efficiency not included in the simulation. The factor of 1/2 is included because both B^+ and B^- mesons are detected, while we report the cross section is B^+ mesons only.

Table 1: B^+ meson differential cross section from the Run 1 data.

$\langle p_T \rangle$ (GeV/ c)	Events	Acceptance (%)	Cross Section (nb/[GeV/ c])
7.4	160 ± 23	1.70 ± 0.01	$816 \pm 118 (stat) \pm 29 (sys_{uc}) \pm 107 (sys_{fc})$
10.4	114 ± 17	4.44 ± 0.01	$221 \pm 32 (stat) \pm 8 (sys_{uc}) \pm 29 (sys_{fc})$
13.4	62 ± 13	6.93 ± 0.02	$76.7 \pm 15.7 (stat) \pm 2.2 (sys_{uc}) \pm 10.0 (sys_{fc})$
18.2	71 ± 11	9.86 ± 0.04	$18.8 \pm 2.6 (stat) \pm 0.5 (sys_{uc}) \pm 2.5 (sys_{fc})$

Table 1 lists the differential cross section as a function of p_T . The experimental points are plotted at $\langle p_T \rangle$ which is the value of p_T for which the theoretical differential cross section equals the integral over each momentum range. The three errors quoted on the cross section are statistical ($stat$), uncorrelated systematic (sys_{uc}), and fully correlated systematic (sys_{fc}), respectively. The uncorrelated systematic errors include variations of the production and decay kinematics that would affect the determination of the acceptance. The correlated systematic errors include uncertainties that are independent of the B^+ transverse momentum. The largest of these errors is due to limited knowledge of the $B^+ \rightarrow J/\psi K^+$ branching ratio which yields a systematic uncertainty of more than 10%. Figure 1 shows the differential cross section measured at the mean p_T of each bin compared with the next-to-leading order QCD² calculation using the MRST structure functions⁴. The dashed lines indicate the change in the theoretical predictions as the b quark mass is varied between 4.5 and 5.0 GeV/ c , the renormalization scale is varied between $\mu_0/2$ and $2\mu_0$, and the Peterson fragmentation parameter is varied between 0.004 and 0.008. The solid curve is for the central values of these parameters: $m_b = 4.75$ GeV/ c^2 , $\mu_0 = \sqrt{m_b^2 + p_T^2}$, and $\epsilon_P = 0.006$. The fraction of \bar{b} quarks that fragment into B^+ is 37.5%.

The measured total B^+ production cross section for $p_T(B^+) \geq 6.0$ GeV/ c and $|y| \leq 1.0$ is $\sigma_B = 3.52 \pm 0.38(stat + sys_{uc}) \pm 0.48(sys_{fc}) \mu\text{b}$ where the first uncertainty is the sum in quadrature of the statistical and uncorrelated systematic error and the second is the correlated systematic error. The new measurement of the B^+ differential cross section confirms that the absolute rate is higher than the NLO QCD predictions. Higher-order QCD calculations could be crucial to understanding this discrepancy.

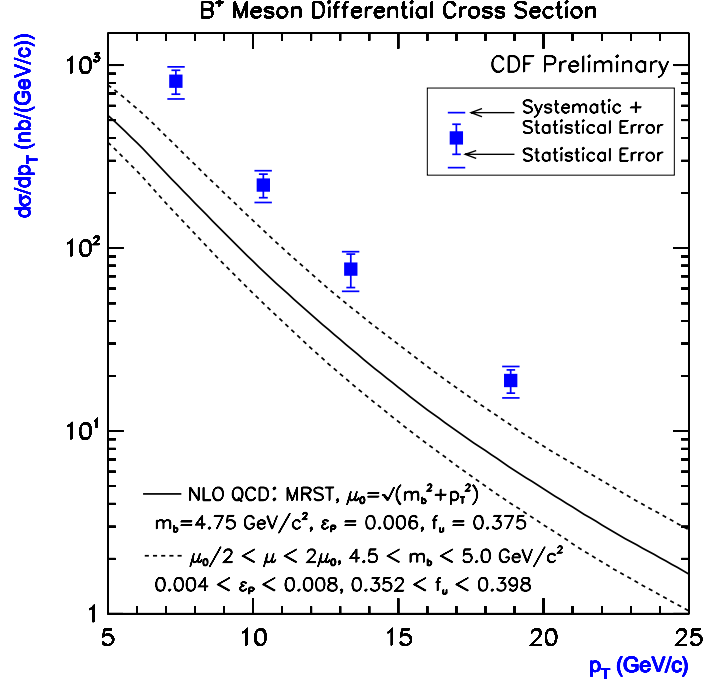


Figure 1: B^+ meson differential cross measurements compared to the theoretical prediction.

4 Searches for radiative penguin decays

Flavor-changing neutral currents are suppressed in the Standard Model (SM) by the Glashow-Iliopolus-Maiani mechanism. Penguin processes result in $b \rightarrow s$ or $b \rightarrow d$ transitions through the emission and reabsorption of a W boson. If a photon is emitted from the loop this results in an "electromagnetic" penguin. The SM penguin diagrams are dominated by the exchange of the top quark. The existence of non-SM charged particles, such as the charged Higgs, could affect the branching ratios and could enhance direct CP-violating effects. Therefore measurements of the radiative penguin decays probe physics beyond the SM. Within the SM framework, the radiative decays are sensitive to the magnitude of the Cabibbo-Kobayashi-Maskawa (CKM) matrix elements $|V_{ts}|$ and $|V_{td}|$.

In 1993, the CLEO collaboration observed the first radiative penguin decays of B mesons. Recently they measured the branching fraction $\mathcal{B}(\bar{B}_d^0 \rightarrow \bar{K}^{*0}\gamma) = (4.55^{+0.72}_{-0.68} \pm 0.34) \times 10^{-5}$ and they reported $\mathcal{B}(B \rightarrow \rho\gamma)/\mathcal{B}(B \rightarrow K^*\gamma) < 0.32$ at a 90 % confidence level (CL). No exclusive decays of the \bar{B}_s^0 or Λ_b have been observed yet. The Delphi collaboration has set a limit on $\mathcal{B}(B_s \rightarrow \phi\gamma) < 7.0 \times 10^{-4}$ at a 90 % CL. CDF has searched for $\bar{B}_d^0 \rightarrow \bar{K}^{*0}(\rightarrow K^-\pi^+)\gamma$, $\bar{B}_s^0 \rightarrow \phi(\rightarrow K^-K^+)\gamma$ and $\Lambda_b \rightarrow \Lambda(\rightarrow p\pi^-)\gamma$ in the Run 1 data sample. Two methods were employed to record radiative decays.

4.1 Method I: Photon Trigger

In the first method (Method I) the photon is detected in the electromagnetic calorimeter by a specialized trigger as a cluster of deposited energies with transverse energy $E_T > 10$ GeV for 22.3 pb^{-1} of Run 1B and $E_T > 6$ GeV for 6.6 pb^{-1} recorded during 1995-1996 (Run 1C). Because of the high trigger rate for such events we recorded only events with two tracks with high transverse momentum ($p_T > 2$ GeV/c). This trigger is very inefficient for the Λ_b radiative decay because the pions from the Λ have a soft transverse momentum distribution.

The B mesons are reconstructed by combining the momentum of the photon and the two tracks, where the two tracks are constrained to intersect at a common point, indicating the decay point of

the B meson candidate. The mass resolution of the reconstructed B meson is around $100 \text{ MeV}/c^2$ and is dominated by the uncertainty in the photon energy measurements of the central electromagnetic calorimeters $\sigma(E_T)/E_T = [(0.137)^2/E_T + (0.02)^2]^{1/2}$ with E_T measured in GeV. The branching fractions are determined by forming the ratio with the known branching fraction for the decay $\mathcal{B}(B \rightarrow e^- D^0 X)$, where the D^0 meson is reconstructed through its decay $D^0 \rightarrow K^- \pi^+$ and X indicates any missing particle. Electrons were collected through the inclusive electron data stream with trigger requirements similar to the ones imposed on the photons of the penguin data set. The topology of the reference channel is similar to the one resulting from the radiative decay and therefore common systematic errors cancel in the ratio of branching fractions. We find 1 $\bar{B}_d^0 \rightarrow \bar{K}^{*0} \gamma$ and 0 $\bar{B}_s^0 \rightarrow \phi \gamma$ candidates. The systematic errors are $\approx 25 \%$ and 31% for the \bar{B}_d and \bar{B}_s respectively and are dominated by the number of events observed for the reference decays, the fraction of D from B decays that are coming from excited D states, the branching fraction of the decay chain $\bar{B} \rightarrow e^- D^0 (\rightarrow K^- \pi^+) X$ and the fragmentation parameters f_d and f_s . The resulting upper limits are 1.6×10^{-4} and 2.1×10^{-4} at a 90 % CL for the \bar{B}_d and \bar{B}_s radiative decays, respectively.

4.2 Method II: Photon Conversions

In the second method, the photon is identified by an electron-positron pair produced through the external photon conversion before the Central Tracking Chamber detector volume. The typical photon conversion probability is 6% for the CDF detector. Conversion electrons with $E_T > 8 \text{ GeV}/c$ served as a trigger for recording these events in 75 pb^{-1} of data collected during Run 1B. The photon conversion candidate is formed by the trigger electron and an oppositely charged track with $p_T > 0.5 \text{ GeV}/c$. The B meson (\bar{B}_s^0, \bar{B}_d^0) candidate is formed by the photon conversion candidate and a pair of oppositely charged tracks reconstructed in the SVX. A fit is performed with the constraints that the meson tracks come from a common vertex, the photon conversion candidate points back to the B meson decay vertex and the four-track system points back to the primary vertex. The typical mass resolution of the reconstructed b hadrons is $45 \text{ MeV}/c^2$. We improve the sample purity by requiring the proper lifetime of the B hadron candidate event to be larger than $100 \mu\text{m}$.

Different selection criteria were developed for increasing the sensitivity for the decay $\Lambda_b \rightarrow \Lambda (\rightarrow p \pi^-) \gamma$. Since the Λ has a long lifetime ($c\tau \approx 8 \text{ cm}$), it decays outside the SVX fiducial volume $\approx 85 \%$ of the time. Therefore we reconstruct the Λ candidates using two oppositely charged CTC tracks. We find 2 candidates in the Λ_b signal region and an expected background of 3.4 ± 0.6 events.

To determine the branching ratios we use the decay $B_u^- \rightarrow J/\psi (\rightarrow e^+ e^-) K^-$ as reference. The systematic uncertainties for the \bar{B}_d^0 , \bar{B}_s^0 and the Λ_b decays are 26 %, 29 %, and 43% respectively. The systematic error is dominated by the statistics of the reference channel, the branching fractions, and the conversion probability. The upper limits on the branching fractions for the decays $\bar{B}_d^0 \rightarrow \bar{K}^{*0} \gamma$, $\bar{B}_s^0 \rightarrow \phi \gamma$, and $\Lambda_b \rightarrow \Lambda \gamma$ are 1.9×10^{-4} , 2.5×10^{-4} , and 6.5×10^{-4} at a 90 % CL.

4.3 Combined Results

Since the two analysis methods used for the decays of the \bar{B}_d^0 and the \bar{B}_s^0 are statistically independent we add the number of candidates found in each analysis. There are 2 \bar{B}_d^0 and 0 \bar{B}_s^0 candidates with an expected background of 0.6 ± 0.3 and 0.1 ± 0.1 respectively. The uncorrelated systematic uncertainties are added in quadrature; the fully-correlated systematic uncertainties are summed. The combined systematic uncertainties are 18 % and 25 % for the $\bar{B}_d^0 \rightarrow \bar{K}^{*0} \gamma$ and the $\bar{B}_s^0 \rightarrow \phi \gamma$ decays respectively. The upper limits are estimated without background subtraction. For the decays $\bar{B}_d^0 \rightarrow \bar{K}^{*0} \gamma$ and $\bar{B}_s^0 \rightarrow \phi \gamma$ we obtain 1.1×10^{-4} and 1.2×10^{-4} at a 90 % CL.

5 The measurement of $\sin 2\beta$

CDF exploits the large B cross section at the Tevatron to obtain a large sample of $J/\psi K_S^0$ decays to measure $\sin 2\beta$. The analysis reported here uses the entire Run I data sample of 110 pb^{-1} and is described in detail elsewhere⁵. The J/ψ sample is identified by selecting two oppositely charged muon

candidates each with $p_T > 1.4$ GeV/c. The K_S^0 candidates are found by matching oppositely charged tracks assumed to be pions. The K_S^0 candidates are required to have $p_T(K_S^0) > 700$ MeV/c and to travel a significant distance from the primary vertex. The $\mu^+\mu^-$ and $\pi^+\pi^-$ are constrained to the appropriate masses and separate decay vertices. A K_S^0 candidate is constrained to point back to the B^0 meson decay point and then the B^0 meson candidate is constrained to point back to the primary vertex. To further improve the signal-to-background ratio, B candidates are required to have $p_T(B)$ above 4.5 GeV/c.

The data are divided into two samples which are called SVX and non-SVX samples. The SVX sample requires both muon candidates to be well measured by the silicon vertex detectors. The B candidates in this sample have a proper decay time resolution of $\sigma_{ct} \approx 60$ μm . The non-SVX sample contains events in which one or both of the muon candidates are not measured in the silicon vertex detector. B candidates in this sample have a low proper decay time resolution of $\sigma_{ct} \approx 300 - 900$ μm . The SVX sample and the non-SVX sample contain 202 ± 18 and 193 ± 26 events respectively. The SVX subsample was used for a previous measurement of $\sin 2\beta^{10}$.

5.1 Flavor tagging

In order to observe the CP asymmetry, A_{CP} , we must determine the b flavor at production by establishing if the B meson contains a b or a \bar{b} quark. Since the error on $\sin 2\beta$ depends on $1/\sqrt{\epsilon D^2 N}$ we can improve the statistical reach by using several taggers. CDF has studied three tagging algorithms to measure Δm_d in $B^0 - \bar{B}^0$ oscillations. Two are opposite side tag algorithms and one is a same side tag algorithm. The two opposite side tagging algorithms, the soft lepton tag (SLT) and the jet-charge tag (JETQ), identify the flavor of the *opposite* B in the event at the time of production. The dilution parameters for all tagging algorithms are measured on calibration samples. At the Tevatron the strong interaction creates $b\bar{b}$ pairs at sufficiently high energy that the B mesons are largely uncorrelated. For example, the b quark could hadronize as a \bar{B}^0 while the \bar{b} could hadronize as a B^+ , B^0 , or B_s^0 meson. Therefore we can use a sample of 998 ± 51 $B^\pm \rightarrow J/\psi K^\pm$ decays to measure the tagging dilutions for the opposite side algorithms. The performance of the same side tagging methods is evaluated using a high statistic sample of approximately 6,000 $B \rightarrow \nu \ell D^{(*)}$ decays and in lower statistics sample $B \rightarrow J/\psi K^{*0}$ (≈ 450 events).

The same side tagging method, or SST⁷, relies on the correlation between the B flavor and the charge of a nearby particle. Such a correlation can arise from the fragmentation processes which form a B meson from a \bar{b} quark and from the decay of an excited B meson state (B^{**}). During the fragmentation a \bar{b} quark forming a B^0 can combine with a d leaving a \bar{d} which can form a π^+ with a u quark from the sea. The excited B state will decay $B^{**+} \rightarrow B^{(*)0} \pi^+$. Therefore in both cases a B^0 (\bar{B}^0) meson is associated with a positive (negative) particle respectively. The dilution of the SST sample was measured, using the SVX sample, in the large $B \rightarrow \ell D^{(*)} X$ data sample to be $D = (16.6 \pm 2.2)$ %. A Monte Carlo simulation was used to extrapolate the dilution from the momentum range of B mesons in semileptonic decays, which have an average p_T of 21 GeV/c, to the lower B momentum of the $B \rightarrow J/\psi K_S^0$ sample with an average p_T of 12 GeV/c. The dilution in the non-SVX sample is $D = (17.4 \pm 3.6)$ %.

The soft lepton tag⁸ associates the charge of the lepton (e or μ) from semileptonic decays with the flavor of the parent B meson because $b \rightarrow \ell^-$. Since we are tagging the opposite B meson, its flavor is anti-correlated with the flavor of the B-meson that decays to $J/\psi K_S^0$. Hence a $\ell^-(\ell^+)$ tags a B^0 (\bar{B}^0) decaying as $B \rightarrow J/\psi K_S^0$. The dilution of the SLT tagging method is measured by applying the SLT algorithm to the $B^\pm \rightarrow J/\psi K^\pm$ data sample. We find $D = (62.5 \pm 14.6)$ %.

The other opposite side method, "Jet charge", or JETQ, tags the b flavor by measuring the average charge Q of the opposite side jet. A B^0 (\bar{B}^0) is selected by $Q_{jet} < -0.2$ (> 0.2). If the jet charge $|Q_{jet}| < 0.2$ then the jet is considered untagged. The dilution $D = (23.5 \pm 6.9)$ % is found by applying the JETQ algorithm to the $B^\pm \rightarrow J/\psi K^\pm$ data sample.

The performances of the individual tagging methods are comparable, as summarized in table 2. The three tagging methods are combined to reduce the uncertainty in the CP asymmetry. The combined

tagging power is $\epsilon D^2 = (6.3 \pm 1.7) \%$, and the efficiency for flavor tagging a $J/\psi K_S^0$ with a least one tag is $\approx 80 \%$.

Table 2: Summary of the tagging algorithms performance. All numbers are in percent. The efficiencies are obtained from the $B \rightarrow J/\psi K_S^0$ sample. The dilution parameters are derived from the $B^\pm \rightarrow J/\psi K^\pm$ sample.

Tagging method	ϵ	Dilution
SST SVX	35.5 ± 3.7	16.6 ± 2.2
SST non-SVX	38.1 ± 3.9	17.4 ± 3.6
SLT all	5.6 ± 1.8	62.5 ± 14.6
JETQ all	40.2 ± 3.9	23.5 ± 6.9

6 The measurement of $\sin(2\beta)$

An unbinned likelihood fit is used to determine $\sin 2\beta$. The parameters in the fit can be described as a vector with 65 components. The value of $\sin(2\beta)$ is a free parameter of the fit while the remaining 64 parameters describe other features of the data. The likelihood function is described in detail in ⁵.

The fit yields $\sin(2\beta) = 0.79^{+0.41}_{-0.44}$ (*stat.* + *syst.*) The asymmetry is shown in figure 4 for the SVX and non-SVX events separately. The asymmetry for the SVX events which have good ct resolution is shown as a function of the proper lifetime. The lifetime information for the non-SVX events is utilized in the fit but the time-integrated asymmetry is shown in figure 4 because the decay length information has low resolution. The data shown in figure 4 has been side-band subtracted. The curves displayed in the plot are the results of the full maximum likelihood fit using all the data.

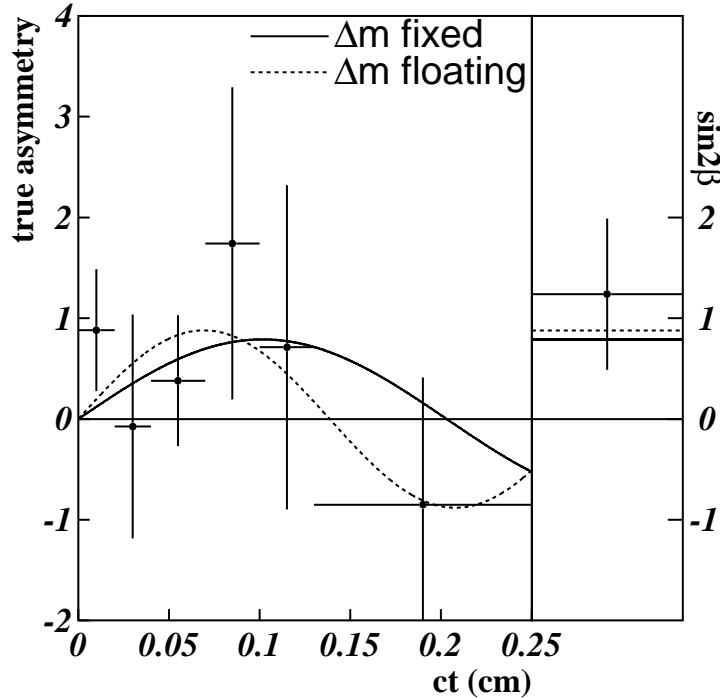


Figure 2: The true asymmetry as a function of time for $J/\psi K_S^0$ events. The data points are side-band subtracted and have been combined according to the effective dilutions for single and double tags. The time integrated asymmetry for non-SVX events are shown on the right.

A scan of the likelihood function can be used to determine whether the CDF result supports $\sin(2\beta) > 0$. Using the Feldman-Cousin frequentist approach⁹ we determine $0.0 < \sin 2\beta < 1$ at 93 % confidence level. The Bayesian method assumes a flat prior probability in $\sin(2\beta)$ and yields $\sin(2\beta) > 0$ at 95 % confidence level. This is the first compelling evidence for CP violation in B meson decays.

7 Future Expectations

The CDF experiment is undergoing upgrades to improve the performance of the detectors for the upcoming data taking that will begin in March 2001. The main injector will increase the production rate of antiprotons by approximately a factor of three over the rates in Run I. This improvement will yield higher instantaneous luminosity. At the beginning of Run II (Run IIA) the number of proton bunches will increase from 6 to 36 and the bunches will collide every 396 ns. During this stage CDF expects to collect about 2 fb^{-1} . Later, in Run IIB, the machine will operate with 100 bunches with collisions every 132 ns. The total Run II luminosity is expected to be about 15 fb^{-1} .

CDF will have a new eight layer silicon vertex detector that extends from a radius of 1.6 cm to 28 cm from the beam line. The layer close to the beam line (L00) is instrumented with single sided sensors with a radiation-hard multi-guard-ring design that allows operation at high voltages. The remaining seven layers have double sided sensors that allow track reconstruction in three dimensions. The impact parameter resolution expected in Run II is $5.5 + 17 \mu\text{m}/p_T$ with p_T in GeV/c . A new drift chamber (COT) has a drift time a factor of eight faster than in Run I. A new scintillating tile calorimeter will be inserted in the pseudorapidity region $|\eta| > 1$. In the muon system some gaps in the region $|\eta| < 1$ will be filled and a new muon system has been built for the region $1.0 < |\eta| < 1.5$. A new time-of-flight detector (TOF) with expected time resolution of 100 ps is being built which will allow 2σ K/π separation for tracks with momentum less than $1.6 \text{ GeV}/c$.

CDF will continue investigating B physics in Run II. CDF is expected to collect 10,000 $B^0/\bar{B}^0 \rightarrow J/\psi K_S^0$ decays where $J/\psi \rightarrow \mu^+\mu^-$ and $K_S^0 \rightarrow \pi^-\pi^+$. A further increase in the number of events is expected from triggering on $J/\psi \rightarrow e^+e^-$ and from the higher production b cross section at $\sqrt{s} = 2 \text{ TeV}$. The B flavor tags will be calibrated on a sample of 40,000 $B^+ \rightarrow J\psi K^-$ decays and 20,000 $B^0/\bar{B}^0 \rightarrow J/\psi K^{*0}$ decays. The expected combined flavor tagging effectiveness based on same side tagging, soft lepton tagging and jet charge is 6.7 % which yields an error $\delta(\sin 2\beta) = 0.084$. The TOF will make it possible to use a new kaon flavor tag since the decay of b hadrons containing $b(\bar{b})$ quarks usually produce $K^+(K^-)$. With this additional flavor tag the combined tag effectiveness could increase to 9.1 %.

A new displaced vertex trigger at Level II (SVT) would allow triggering on hadronic B decays such as $B \rightarrow \pi^+\pi^-$ and $B^0 \rightarrow K^-\pi^+$. The $B^0 \rightarrow \pi^+\pi^-$ signal yield is obtained from a Monte Carlo simulation. Assuming the branching fraction $\mathcal{B}(B^0 \rightarrow \pi^+\pi^-) = (4.7_{-1.5}^{+1.8} \pm 0.6) \times 10^{-6}$, CDF expects 4,000-7,000 events in 2 fb^{-1} of data. Assuming a signal-to-background ratio of 1:4, ϵd^2 of 9.1 %, and a sample of 4,700 $B^0/\bar{B}^0 \rightarrow \pi^+\pi^-$ decays, CDF expects to measure the CP asymmetry with an uncertainty of 0.13. The extraction of $\sin 2\alpha$ from the measured time dependence requires the determination of penguin contributions.

The CP asymmetry in $B_s^0 \rightarrow J/\psi\phi$ measures the phase in V_{ts} which is expected to be very small in the SM. Therefore the observation of large CP asymmetries in this mode would indicate new physics. Based on the Run I data we expect the data yield for $B_s^0 \rightarrow J/\psi\phi$ to be about 60% of the data yield for $B_d^0 \rightarrow J/\psi K_S^0$.

CDF is studying the determination of $\sin \gamma$ through the decays $B_s^0 \rightarrow D_s^- K^+$ and $B^\pm \rightarrow DK^\pm$. In 2 fb^{-1} of data we expect about 700 $B_s^0 \rightarrow D_s^- K^+$ signal events before flavor tagging. This channel suffers from the physics background $B_s^0 \rightarrow D_s^- \pi^+$, which is ten times larger. Preliminary studies using dE/dx , TOF, and the excellent mass resolution of the COT indicate that CDF should achieve a signal-to-background ratio of 1:1. The combinatorial background is expected to yield a signal-to-background ratio of about 1:5. The reach for γ is determined by fitting $\sin(\gamma + \delta)$ where δ is the strong phase. We estimate an uncertainty for $\sin(\gamma + \delta)$ of 0.43 (0.79) for a signal-to-background ratio of 1:1 (1:6).

Rare B decays provide a stringent test of the Standard Model and could be sensitive to new physics.

We expect between 100 to 300 $B^\pm \rightarrow \mu^+ \mu^- K^\pm$ and between 400 and 1100 $B^0 \rightarrow \mu^+ \mu^- K^{*0}$. This will enable CDF to study the invariant mass distribution of the dimuon pairs and the forward-backward charge asymmetry in the decay. Both such distribution are sensitive to new physics.

In the Standard Model, $B_s^0 \bar{B}_s^0$ oscillations occur through the top quark contributions to the box diagram. The size of the mixing is expressed in terms of the parameter $x_s = \Delta m_s \tau(B_s^0)$ which relates the mass difference between the two mass eigenstates and the average lifetime of the states. The B_s^0 decay modes used in the CDF studies are $B_s^0 \rightarrow D_s \pi^+$ and $B_s^0 \rightarrow D_s \pi^+ \pi^- \pi^+$, where the D_s^- is reconstructed as $\phi \pi^-$ or $K^+ K^-$. We expect 7,200-10,600 events in the $D_s \pi^+$ and 8,100-12,800 in $D_s \pi^+ \pi^- \pi^+$. To estimate the reach in x_s we vary the total number of events in these two decay modes from 5,000 to 30,000 and we vary the signal-to-background ratio between 1:2 and 2:1. The silicon system will provide a proper time resolution of 45 ps and the TOF will increase the tagging effectiveness to 11.3 %. CDF is expected to provide a 5 σ measurement of x_s up to 63 if the signal-to-background ratio is 2:1 and 56 if the signal-to-background ratio is 1:2. The currently favored Standard Model value of x_s is in the range 18 to 27 with a 90 % CL limit of $x_s < 31$. Therefore CDF covers the expected Standard Model range.

8 Conclusions

The large production rate of heavy quarks at hadron colliders has allowed the CDF experiment at the Tevatron to develop a b -physics program highly competitive with those of $e^+ e^-$ experiments. For example, CDF has provided the first measurement of CP violation in the b -system¹⁰, precisely determined the b hadron lifetimes¹¹ and the neutral B meson oscillation parameters¹². The main goals of the b physics program in Run II are the measurements of the unitarity triangle as well as to exploit the B_s and B_c mesons and the Λ_b baryon which will be unique features of hadron colliders.

In conclusion, hadron colliders will continue to play a crucial role in future studies of b quark systems with the commissioning of the upgraded Tevatron and the upgraded CDF detector.

References

1. CDF Collaboration, F. Abe et al., *Nucl. Instrum. Meth. A* **271**, 387 (1988); CDF Collaboration, F. Abe et al., *Phys. Rev. D* **50** (1994) 2966; D. Amidei et al., *Nucl. Instr. Meth. A* **350**, 73, (1994); P. Azzi et al., *Nucl. Instr. Meth. A* **360**, 137 (1995).
2. Nason *et al.*, *Nucl. Phys. B* **327**, 49 (1989), erratum *ibid.* B **335**, 260 (1990); Beeneker *et al.*, *Nucl. Phys. B* **351**, 505 (1991).
3. CDF collaboration, F. Abe *et al.*, *Phys. Rev. Lett.* **75**, 1451 (1995).
4. A. Martin, W. Stirling and R. Roberts, *Phys. Lett. B* **306**, 145 (1993); *Phys. Lett. B* **443**, 301 (1998); *Eur. Phys. J. C* **4**, 463 (1998).
5. T. Affolder *et al.*, *Phys. Rev. D* **61**, 072005 (2000).
6. Particle Data Group, C. Caso *et al.*, *Eur. Phys. J. C* **C3**(1998) 1.
7. F. Abe *et al.*, *Phys. Rev. Lett.* **80**, 2057 (1998).
8. T. Affolder *et al.*, *Phys. Rev. D* **60**, 112004 (1999).
9. G. J. Feldman and R.D Cousins, *Phys. Rev. D* **57**, 3873 (1998).
10. CDF collaboration, F. Abe *et al.*, *Phys. Rev. Lett.* **81**, 5513 (1998).
11. CDF collaboration, F. Abe *et al.*, *Phys. Rev. D* **57**, 5382 (1998); *Phys. Rev. D* **59**, 032004 (1999); *Phys. Rev. D* **58**, 092002 (1998).
12. CDF collaboration, F. Abe *et al.*, *Phys. Rev. D* **60**, 072003 (1999); *Phys. Rev. D* **60**, 051101 (1999); *Phys. Rev. D* **59**, 032001 (1999).